Available online at www.sciencedirect.com
SCIENCE DIRECT®
International Journal of Heat and Fluid Flow 25 (2004) 864–874
International Journal of HEAT AND FLUID FLOW
www.elsevier.com/locate/ijhff

Application of a PDF method for the statistical processing of experimental data

O. Heinz, B. Ilyushin, D. Markovich *

Institute of Thermophysics, Siberian Branch of Russian Academy of Sciences, Lavrentyev Avenue 1, Novosibirsk 630090, Russia

Received 18 February 2004; accepted 27 May 2004
Available online 6 July 2004

Abstract

A new method of experimental data validation for turbulent flows has been developed and tested. The method is based on the statistical analysis of the ensemble of measured physical quantities. The assumption of the exponential decay of PDF tails for turbulent fluctuations is taken as the basis. The possibility of the PDF for turbulent fluctuations being substantially non-Gaussian has been taken into account. The method developed has been applied to a PIV-measured ensemble of instantaneous velocity fields in a turbulent impinging jet processed by different primary validation methods. Such an approach allows the rejection of the large-amplitude erroneous velocity vectors and corrects the calculation of higher order statistical moments.

Keywords: Experimental data validation; Higher order moments; Coherent structures; PIV; PDF

1. Introduction

The problem of the correct removal of non-physical magnitudes of characteristics measured by different experimental techniques becomes extremely important when the calculation of quantities containing high powers of measured values is of interest. For such cases, even small number of large-amplitude "outliers" (relatively to the whole measured statistics) could result in large errors in the calculated higher order statistical moments. Higher order moments of turbulent flow characteristics are often to be examined in turbulence research. Thus, in second-order closures of the Reynolds stress equations different approaches are adopted for the unclosed terms, particularly the triple moments (see, for example, Dekeyser and Launder, 1983). Such train of closure models can be expanded to higher statistical moments and the possibility of success depends, besides, on the availability of proper experimental information. At times one needs to verify theoretically derived relationships between correlations of different orders and also in estimating the turbulent kinetic energy budget.

The measurements of higher order statistical moments of turbulent flow characteristics are not extensive. For wall shear flows a summary of collected data on measurements of higher order moments is presented in the paper of Jovanovich et al. (1993). The most cited data are obtained with the aid of the hot-wire anemometer (HWA) and represent single-point correlations. HWA also was applied by Panchapakesan and Lumley (1993) for diagnostics of free air and helium jets, where combined single-point moments up to fourth order have been measured to characterize turbulent transport. The measurements performed allowed the examination of the satisfactoriness of different triple moment models for the fully turbulent region of free jet flow. Moreover, in this work on the basis of a literature analysis the conclusion was reached that magnitudes of measured higher order moments substantially depended on the experimental technique used. The main reason for this was supposed to be the errors in the application of experimental methods. A few works devoted to

* Corresponding author. Tel.: +7-3832-344-040; fax: +7-3832-343-480.
E-mail address: dmark@itp.nsc.ru (D. Markovich).

0142-727X/$ - see front matter © 2004 Elsevier Inc. All rights reserved.
doi:10.1016/j.ijheatfluidflow.2004.05.009

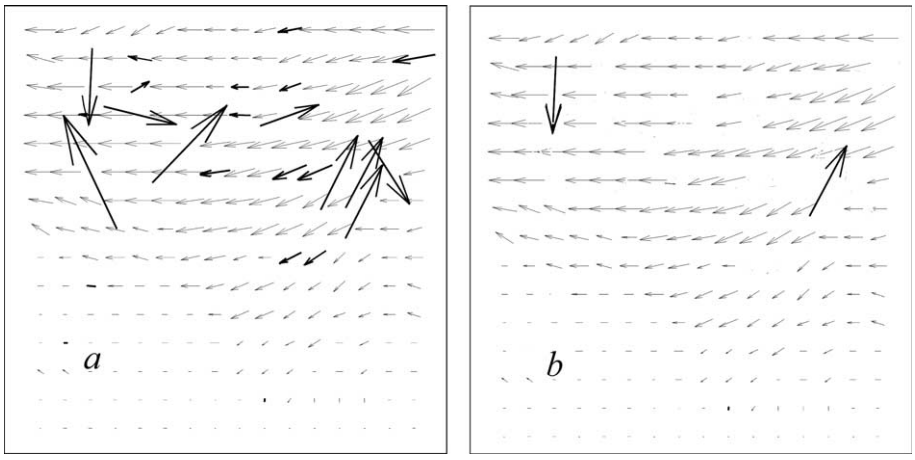

Fig. 1. Velocity fields measured by PIV. (a) Raw velocity field and (b) velocity field after application of primary validation procedures.

measurements in wall-bounded flows was done with the aid of LDA (Keck, 1978; Karlsson and Johansson, 1988). The use of LDA as a non-intrusive method for measurements of higher order moments is acknowledged by a number of authors as preferable in comparison with HWA.

The most modern non-intrusive method for fluid flow diagnostics is definitely PIV. This method allows one to obtain not only single-point correlations of high order but also a large number of spatial correlations. Such information is extremely valuable for the development of advanced models for turbulent flows. At the same time experimental information on the single-point and multi-point higher order moments measured by PIV is absent from the literature.

The application of the PIV technique for studying the statistical structure of turbulent flows assumes the following sequence of operations to be fulfilled: image evaluation, several validation tests for removing outliers and, as a final step, the statistical processing of the determined ensemble of instantaneous velocity fields (Raffel et al., 1998). Intermediate procedures for rejecting outliers (after some chosen approach for correlation-peak detection and validation) are usually based on the analysis of the spatial velocity distribution for each time instant. Most prevalent among these are: the procedure of range validation (cutting off all the velocity vectors which exceed a prescribed threshold for physically realizable values in tested flow) and different methods of spatial filtration based on the local smoothness and differentiability of spatial velocity distributions. The first class of filtration methods does not allow the removal of all outliers without any a priori knowledge about the flow structure. The second approach works rather well in a number of cases. However, it can be correctly applied only at very high spatial resolution of used PIV release. Thus, the "dynamic mean value" and "local median test" methods cannot be used properly in regions with high velocity gradients (especially in the vicinity of shocks) or in regions where it is not possible to calculate average value of neighboring vectors (the presence of clusters of outliers or vicinity of the data field edge).

Fig. 1 shows two stages in the evaluation of velocity field measured by PIV technique: the raw vector field before application of any validation procedure (a) and after application of the complete set of standard and advanced validation algorithms (b). This indicates that, for most cases, some small number of erroneous velocity vectors will always remain in the measured distributions. A more specific example is shown in Fig. 2 where the histograms for fluctuations of the radial velocity component in the given spatial point (at the center of the mixing layer of a submerged axisymmetric jet) are presented. Fig. 2a shows the result of applying a standard range validation procedure. The ensemble of realizations consists of 20,000 instantaneous velocity fields. It follows from the figure that after such filtration the non-physical tails remain in the ensemble (shown by arrows). Although the number of non-rejected outliers is not large (the mean velocity value and velocity variance are almost insensitive to them because of the large array of data), the calculated higher order moments are substantially higher than the true values: the skewness factor (third moment) by seven times and kurtosis (fourth moment) by 18 times, i.e., they are qualitatively incorrect. The corresponding comparisons are made below. As an example of a "true" PDF, the distribution in Fig. 2b is shown.

The main goal of the present paper is the development of an optimal filtration method based on an analysis of large statistical ensembles of velocity fields. With this goal the algorithm for the adequate approximation of the velocity-fluctuation PDF for each spatial point of the flow is built as the basis for correctly cutting the non-physical tails.

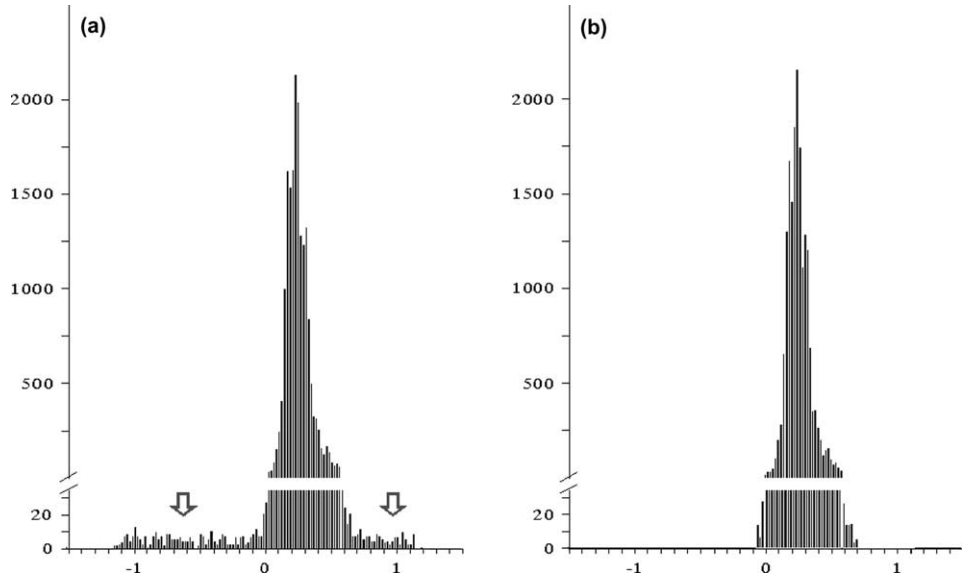

Fig. 2. Histograms for ensemble of radial velocity fluctuations in mixing layer of an axisymmetric jet. (a) Before applying filtering and (b) after applying filtering.

2. Algorithm of basic PDF construction

As the basis of the statistical filtration method, the construction of a basic function (the approximation of the real PDF) with exponential decay of the tails is used. This procedure rests on taking into account the physical essence of the testing flow and has to reflect its statistical structure. The assumption is made that for substantially non-Gaussian distributions (large values of skewness factors and kurtosis) the shape of PDF distribution is influenced in a general degree by vortex formations from the large-wave interval of turbulent spectrum. This assumption is considered as valid because the turbulent pulsations from the inertial interval obey the Kolmogoroff universal statistical law with normal distribution of probabilities, and the dissipation range contains only a small part of the turbulent energy. As a first step towards constructing the basic PDF, the Gauss distribution is considered with known values of first and second statistical moments (mean value and variance). However, if the ensemble of realizations is found to be substantially non-Gaussian, the second step in the PDF construction assumes the use of another distribution. In this new distribution the following properties have to be realized: exponentially decaying tails; accounting for the asymmetry of the ensemble studied (which generally results from vortex structures); an analytical form (for effective use during the processing of large arrays of data).

Such PDF of turbulent fluctuations of the velocity radial or vertical component is represented as a superposition of two independent distributions: an inertial region of the turbulence spectrum (background turbulence) $P_b(u)$ and a large-wave region of the PDF spectrum $P_c(v)$. Here u and v are, respectively, the vertical velocity fluctuations of the background turbulence and the vertical velocity field of coherent structures (Ilyushin, 2001):

$$P(u,v) = P_b(u)P_c(v) = \underbrace{\frac{1}{2\pi\sigma_b}\exp\left\{-\frac{u^2}{2\sigma_b^2}\right\}}_{\text{background turbulence PDF}} \underbrace{\left[\underbrace{\frac{a^+}{\sigma_c^+}\exp\left\{-\frac{(m^+-v)^2}{2(\sigma_c^+)^2}\right\}}_{\text{upflow}} + \underbrace{\frac{a^-}{\sigma_c^-}\exp\left\{-\frac{(m^--v)^2}{2(\sigma_c^-)^2}\right\}}_{\text{downflow}}\right]}_{\text{large scale eddy formation PDF}}, \quad (1)$$

where σ_b^2 is the dispersion of background turbulence; a^+ and a^- are the weighting coefficients, $(\sigma_c^+)^2$ and $(\sigma_c^-)^2$ are the dispersions, m^+ and m^- are the centers of distributions of upflow and downflow of coherent structures. Considering the total turbulent velocity fluctuation, w, as the sum of u and v, one can obtain the total PDF:

$$P(w) = \int_R P(u,v)\delta(w-u-v)\,\mathrm{d}u\,\mathrm{d}v = \frac{a^+}{2\pi\sigma_+}\exp\left\{-\frac{(m^+-w)^2}{2\sigma_+^2}\right\} + \frac{a^-}{2\pi\sigma_-}\exp\left\{-\frac{(m^--w)^2}{2\sigma_-^2}\right\}, \quad (2)$$

where $\sigma_+^2 = \left(\sigma_c^+\right)^2 + \sigma_b^2, \sigma_-^2 = \left(\sigma_c^-\right)^2 + \sigma_b^2$.

From the conditions

$$\int_R P(w)\,\mathrm{d}w = 1, \quad \int_R wP(w)\,\mathrm{d}w = 0, \quad \int_R w^2P(w)\,\mathrm{d}w = \langle w^2\rangle, \quad \int_R w^3P(w)\,\mathrm{d}w = S_w\sigma^3, \quad (3)$$

($\sigma = \langle w^2\rangle^{1/2}$ is the variance and $S_w = \langle w^3\rangle/\langle w^2\rangle^{3/2}$ is the skewness factor) the connections for a^+, a^-, σ_+^2, σ_-^2, m^+ and m^- are the following:

$$\begin{aligned} &a^+ + a^- = 1,\\ &a^+m^+ + a^-m^- = 0,\\ &a^+[(m^+)^2 + \sigma_+^2] + a^+[(m^+)^2 + \sigma_-^2] = \sigma^2,\\ &a^+[(m^+)^3 + 3m^+\sigma_+^2] + a^-[(m^-)^3 + 3m^-\sigma_-^2] = S_w\sigma^3. \end{aligned} \quad (4)$$

The conditions for σ_+^2 and σ_-^2 are found from the assumption that the square of the dispersions σ_+^2 and σ_-^2 are equal to the respective square of the centers of distribution $(m^+)^2$ and $(m^-)^2$ (De Baas et al., 1986):

$$\sigma_+^2 = (m^+)^2, \quad \sigma_-^2 = (m^-)^2. \quad (5)$$

This assumption means that flux directed positively (negatively) remains mainly positive (negative) taking into account possible scatter. The necessary condition for closure of the equation set (for σ_b) is found from the wavelet model (Tennekes and Lumley, 1972). Here the supposition is used that the main part of the energy-containing interval of the fluctuation spectrum is defined by a single main wavelet with typical wave number corresponding to the spectrum maximum (see Fig. 3). The simplified eddy with the typical wave number k_v is considered in the form of the localized perturbation of energy in wave number space (wavelet) with energy $E_v = E_v(k_v)\cdot k_v$. This consideration ensures the cascade transfer of turbulent energy from large-scale eddies to dissipative eddies. In the present work the coherent structures in the flow are assumed to be wavelets containing the energy $E_c = a\varepsilon^{2/3}k_{\max}^{-2/3}$ ($a = 1.6 \pm 0.02$ is the Kolmogoroff constant), $k_{\max}$ is the maximum of the spectrum of the turbulent energy (see Fig. 3). The total turbulent energy is equal to

$$E = \sum_{k_{\min}}^{k_{\max}} E_v(k_v) \approx E_v(k_{\max})\sum_{i=0}^{\infty}[3^{-2/3}]^i \approx 2E_c. \quad (6)$$

The analogous result can be obtained by integration over the inertial interval (without accounting for the deviation from the Kolmogoroff spectrum in the dissipation region) from $k_{\max}$ to infinity and with half of the wavelet energy:

$$E \approx \int_{k_{\max}}^{\infty} a\varepsilon^{2/3}k^{-5/3}\,\mathrm{d}k + \frac{1}{2}E_c = 2E_c, \quad (7)$$

or $\sigma_b^2 = E((\sigma_b^2 + \sigma_c^2)/2 = E)$. Regarding this result, $k_{\max}$ is expressed as $k_{\max} = (2a/E)^{3/2}\varepsilon$ and then $\lambda_{\max} = 2\pi/k_{\max}$. We take the value of the ratio $\sigma_b^2/\langle w^2\rangle$ as equal to 1/3 in the mixing layer (Ilyushin, 2001). This simple assumption allows the PDF parameters to be determined analytically (see below). This is important in developing of a program code for the statistical processing of the extremely large databases. So, the necessary condition for the variance of background turbulence σ_b is:

$$\sigma_b^2 = \frac{1}{3}\langle w^2\rangle. \quad (8)$$

Eqs. (4), (5) and (8) on taking account of the sign of values $m^+ > 0$ and $m^- < 0$ (which correspond to upflow and downflow) have the unique solution:

$$\begin{aligned} &m^+ = \frac{\sigma}{4}\left[S + \sqrt{S^2+8}\right]; \quad m^- = \frac{\sigma}{4}\left[S - \sqrt{S^2+8}\right];\\ &a^+ = -\frac{S - \sqrt{S^2+8}}{2\sqrt{S^2+8}}; \quad a^- = \frac{S + \sqrt{S^2+8}}{2\sqrt{S^2+8}};\\ &(\sigma_c^+)^2 = \frac{\sigma^2}{16}\left[S + \sqrt{S^2+8}\right]^2 - \frac{1}{3}\langle w^2\rangle;\\ &(\sigma_c^-)^2 = \frac{\sigma^2}{16}\left[S - \sqrt{S^2+8}\right]^2 - \frac{1}{3}\langle w^2\rangle. \end{aligned} \quad (9)$$

The above algorithm has been initially applied to the numerical modeling of mass transfer in the atmospheric boundary layer by Ilyushin (2001). In the present work we apply this approach to modeling the substantially non-Gaussian PDFs for a measured ensemble of velocity fields.

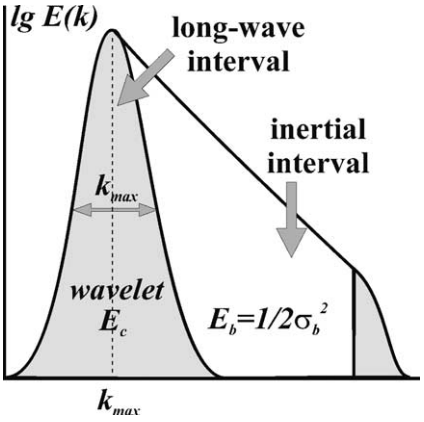

Fig. 3. Representation of the long-wave part of the turbulent fluctuation spectrum as the wavelet.

3. Algorithm of validation

Validation procedure is applied to the ensemble of instantaneous realizations $\phi_{\vec{v}}^N = (\phi_u^N; \phi_v^N) := (u_1 \dots u_N; v_1 \dots v_N)$ of velocity vector components $\vec{v} = (u; v)$. In this paper we consider two-dimensional velocity field. For each spatial point the ensemble ϕ_w^N of instantaneous velocity values is analyzed (w is the velocity component: u or v), the histogram Ψ_N is built for the velocity range $[w_{\min}; w_{\max}]$ with an interval equal to 2Δ (for example, see Fig. 2), where Δ is the accuracy of velocity measurements. The statistical moments are calculated: i.e., the mean value $\langle w \rangle$, the variance $\sigma = \sqrt{\langle w^2 \rangle}$, the skewness factor $S = \langle w^3 \rangle / \sigma^3$ and the kurtosis $E = \langle w^4 \rangle / \sigma^4 - 3$, where

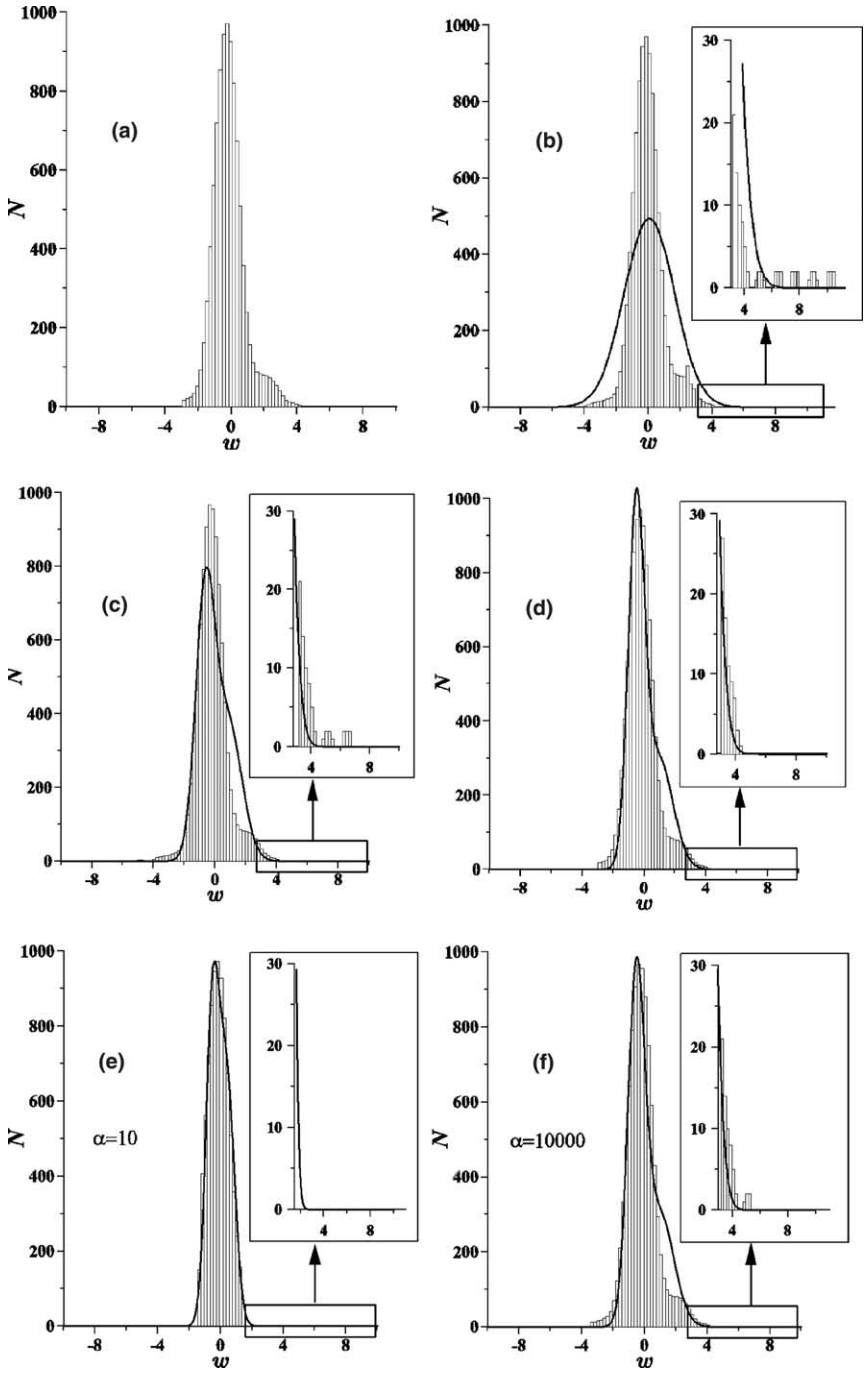

Fig. 4. Histograms and base functions calculated at each step of filtration of an artificial test ensemble with harmonic noise. (a) Initial histogram without noise, (b) first step Gauss approximation, (c) second step – non-Gauss approximation, $\alpha = 1,000$ (d)–(f) final steps of filtration for a equal to 1,000, 10 and 10,000 correspondingly.

$$\langle w\rangle = \frac{1}{N}\sum_{i=1}^{N} w_i, \quad \langle w^2\rangle = \frac{1}{N}\sum_{i=1}^{N}(w_i - \langle w\rangle)^2,$$
$$\langle w^3\rangle = \frac{1}{N}\sum_{i=1}^{N}(w_i - \langle w\rangle)^3, \quad \langle w^4\rangle = \frac{1}{N}\sum_{i=1}^{N}(w_i - \langle w\rangle)^4. \tag{10}$$

On the basis of these parameters the basic function is determined. At the first step the Gaussian distribution is considered:

$$F_1(w) = \frac{1}{\sqrt{2\pi}\sigma}\exp\left\{-\frac{(w-\langle w\rangle)^2}{2\sigma^2}\right\} \tag{11}$$

for the considered velocity interval $[w_{\min}; w_{\max}]$ of the experimentally obtained ensemble. After comparison of the constructed histogram Ψ_N with the first-step basic function $F_1(w)$ it is possible to determine the sub-ensembles $\xi_{w_1}, \xi_{w_2}, \ldots, \xi_{w_k}$ for which the number of realizations with the velocity magnitudes over the range $[w_i - \Delta; w_i + \Delta]$ $i = 1 \ldots N$ exceeds the corresponding value of $F_1(w_i)$ more than α times (the tests with different magnitudes of α will be presented below). Such a procedure is performed for all velocity components. The velocity vector is rejected from the statistical processing for the considered spatial point when each of the velocity components belongs to determined sub-ensembles $\xi_{w_1}, \xi_{w_2}, \ldots, \xi_{w_k}$. The corresponding realizations are not taken into account further. For each subsequent step of filtration the ensemble truncated at the previous step $\phi_{\vec{v}}^M = (\phi_u^M; \phi_v^M) := (u_1 \ldots u_M; v_1 \ldots v_M)$, $M = N - k$ is analyzed according to the algorithm described above. In this case the new function $F_2(w)$ (formula 2) is used as the basic one (instead of the Gaussian), with the parameters (9) calculated according to (10) for the truncated ensemble. This procedure is repeated until the quantity of wrong vectors, defined according such criteria, becomes equal to zero.

4. Testing of algorithm

To test the proposed filtration algorithm the generated ensembles of realizations have been processed with a predetermined distribution $P(w)$ and imposed noise $f(w)$. As a distribution $P(w)$ the Gram–Charlier series, truncated at the third term, was used:

$$P(w) = \frac{1}{\sqrt{2\pi}}\exp\left\{-\frac{w^2}{2}\right\}\left[1 + \frac{1}{3!}S(w^3 - 3w) + \frac{1}{4!}E(w^4 - 6w^2 + 3)\right]. \tag{12}$$

When the parameters E and S are equal to zero, the series (12) represents the Gaussian function.

Table 1
Convergence of the filtration method

Noise amplitude (%)	Noise parameters/ number of iteration	Mean	Variance	Skewness	Kurtosis
0.0 (True distribution)		2.004	0.986	0.457	0.819
1.0	Initial distribution with imposed harmonic noise; $w \in [-10; 10]$	1.936	1.552	−1.864	17.182
	1	1.994	1.119	0.033	3.500
	2	1.997	1.009	0.378	0.833
	3 (final iteration)	2.005	0.998	0.451	0.740
2.0	Initial distribution with imposed white noise; $w \in [-10; 10]$	1.840	1.962	−1.881	11.657
	1	1.985	1.385	−0.098	6.391
	2	1.997	1.102	0.229	1.717
	4 (final iteration)	2.019	1.031	0.504	0.841
	Initial distribution with imposed harmonic noise; $w \in [-5; 15]$	2.212	1.960	2.623	13.339
	1	2.010	1.371	0.337	6.197
	2	2.034	1.113	0.687	1.893
	10 (final iteration)	2.004	1.028	0.430	0.839
4.0	Initial distribution with imposed white noise; $w \in [-10; 10]$	1.683	2.542	−1.547	6.534
	1	1.926	2.019	−0.426	5.742
	2	1.923	1.561	−0.589	4.768
	8 (final iteration)	2.016	1.069	0.422	0.775

Two variants of imposed "noise" $f(w)$ have been tested: the harmonic (13a) and random white noise (13b) additions with amplitude A (varied from 1% to 5% relative to the maximum in the distribution). The noise was imposed onto distribution (12). The wavelength β in the harmonic case was varied in the range $\beta = (0.01 - 0.1)\sigma$, where σ is the variance of $P(w)$:

$$f(w) = A(1 + \sin(\beta w)), \tag{13a}$$

$$f(w) = A\ \mathrm{rand}(w). \tag{13b}$$

The testing procedure includes the calculation of mean values, and the variance, skewness factor and kurtosis for the initial ensemble $P(w)$ without noise. Then the ensemble is assembled for the superposition $P(w) + f(w)$. During filtering all vectors corresponding to subensembles $\xi_w^1, \xi_w^2, \ldots, \xi_w^m$ were considered as spurious and have been rejected. Filtered histograms and corresponding statistical moments were compared with the initial values at each step of the filtering cycle.

Testing of the algorithm was performed for the noise (with different amplitudes and β) imposed both on the Gaussian base distribution and on the different types of non-Gaussian base distributions (12) with various parameters S and E. The range of w where the noise was imposed was also varied. The results showed that developed algorithm corrects the statistical moments with an accuracy up to 10% (when the noise amplitude does not exceed 5%).

The comparison of histograms is presented in Fig. 4 for the case of harmonic noise. The following values of the parameters have been chosen: $S = 0.6$; $E = 2.0$, for Eq. (12) and $A = 0.01$, $\beta = 5$ for (13). The ranges of w for noise superposition consisted of $[-10; 10]$. In Fig. 4a the model base artificial histogram is presented corresponding to the distribution (12). Fig. 4b shows the first iteration of the filtration algorithm – the Gauss approximation – Fig. 4c and d the second and final iterations. As a rule, it is sufficient to adopt up to 5–8 iterations to reach the true values. It is seen that during each step of filtration the noisy additions to the PDF are rejected and the resulting histogram (Fig. 4d) has exponential decay character for the tails.

The determinative parameter of developed algorithm is the coefficient α – the empirical threshold for rejecting vectors. Fig. 4d–f show the sensitivity of the resulting PDF to the magnitude of α. In Fig. 4e the rather rough value ($\alpha = 10$) is applied. The resultant PDF does not contain a substantial part of the physically correct large- and intermediate-amplitude fluctuations. In contrast, Fig. 4f shows a too mild condition, $\alpha = 10,000$. The imposed noise remains in the final PDF. After a set of tests the optimal value of this parameter was found to be $\alpha = 1,000$ (Fig. 4d).

Table 1 shows the numerical representation of convergence of the filtration process, both for the harmonic and the random noise. The first line gives the "true" values for first four moments calculated with the aid of distribution (12) taking account of the discrete (histogram) representation. The several sets of parameters for filtration are presented. Further sections in the table show the evolution of moments with iterations of filtration for different noise parameters: amplitude, type of noise and range of w. The range of w for the imposed noise is not too wide—the "noisy" higher order moments are essentially smaller than in "unfiltered" reality, mentioned in the Introduction, but the chosen range was

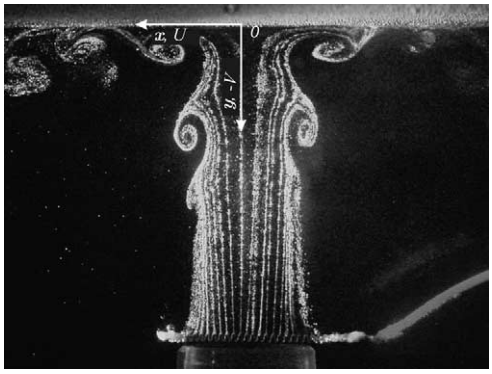

Fig. 5. Photograph of impinging jet flow. $H/D = 3$.

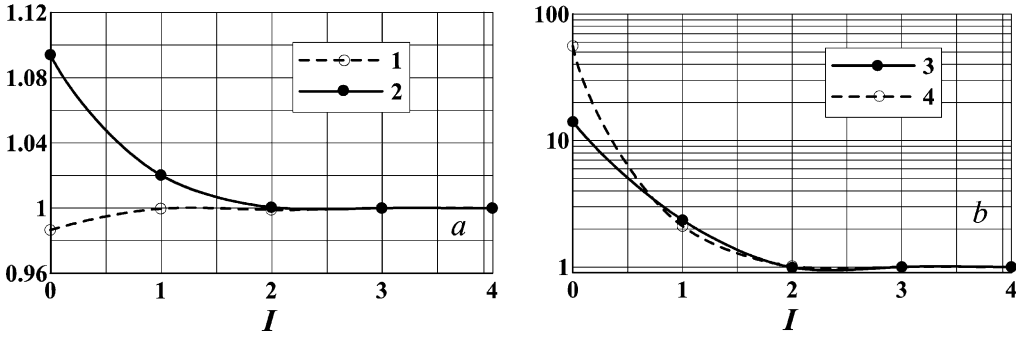

Fig. 6. Related values of statistical moments calculated at different steps of filtration. (a) Mean value, 1 and variance, 2; (b) skewness factor, 3 and kurtosis, 4.

sufficient for testing. It is clearly seen from the table that, during iterative filtration, the statistical moments approach the true values. The convergence becomes somewhat poorer with increasing noise amplitude.

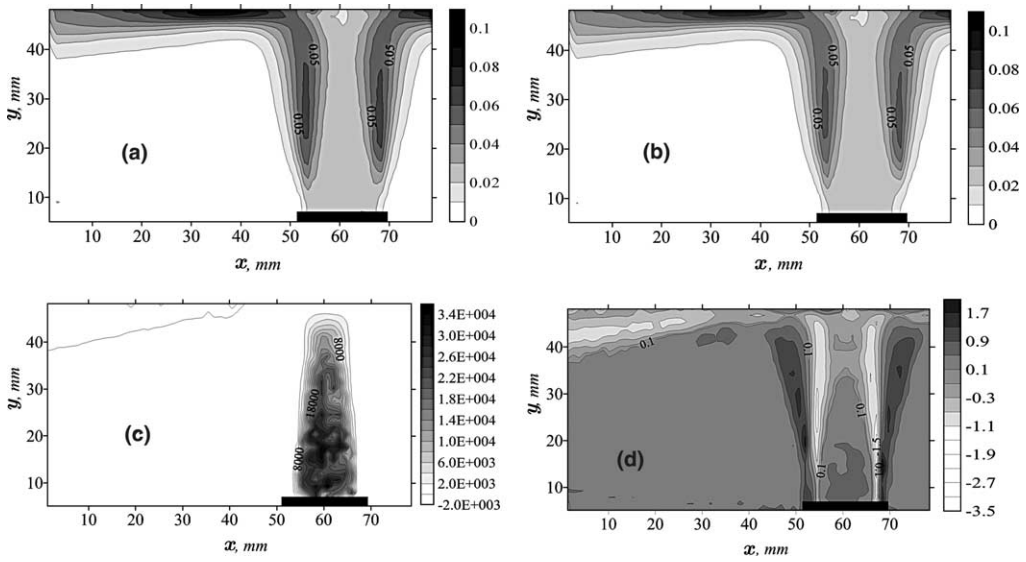

Fig. 7. Calculated distributions of variance and skewness factor in an axisymmetric turbulent impinging jet. (a), (c) σ_u, S_v for non-filtered data; (b), (d) σ_u, S_v for filtered data.

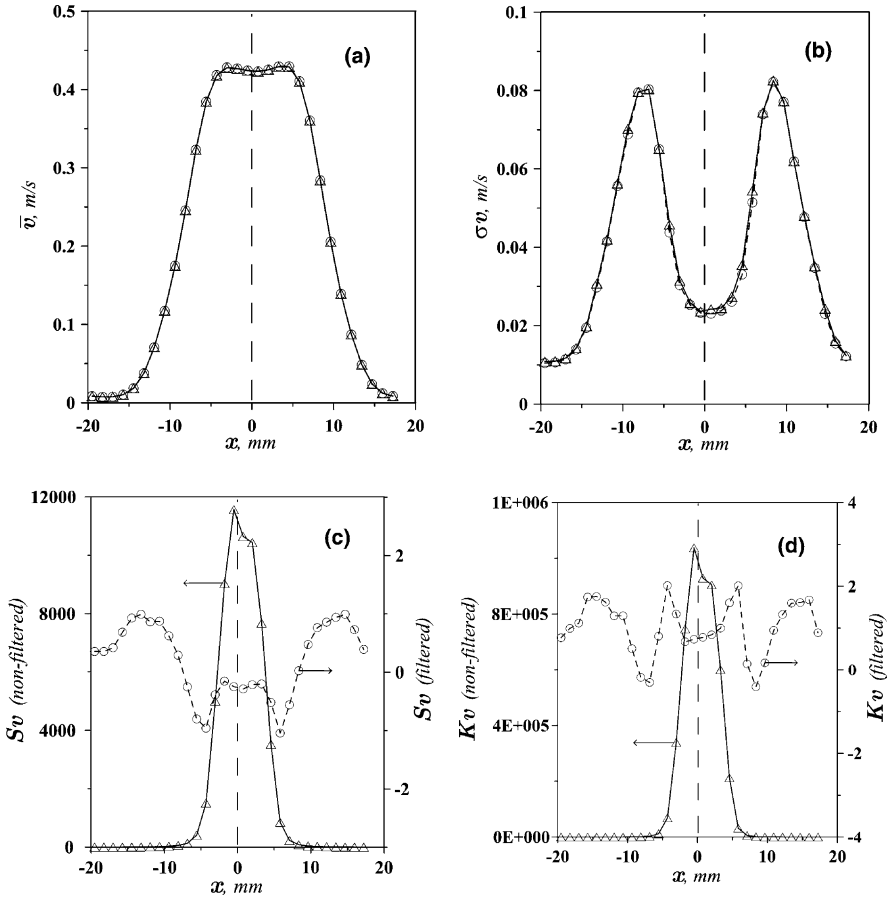

Fig. 8. Distributions of statistical moments across a horizontal cross-section of the impinging jet flow ($y/D = 2$), $\mathscr{R}e = 7600$. (a) Mean longitudinal velocity, (b) its variance, (c) its skewness and (d) its kurtosis. Triangles non-filtered values, circles filtered values.

Nevertheless, the accuracy of the calculated moments of the filtered data remains acceptable since, as has been concluded from the analysis of real experimental data, the amount of erroneous vectors at each histogram bar practically does not exceed 1–2% compared with the maximum of the PDF. Undoubtedly, the filtration procedure does not provide rejection of outliers falling into the range of the main distribution. This fact, however, is not critical, because these outliers do not significantly affect the high order moments.

5. Application of the validation algorithm

The developed algorithm has been applied to the ensemble of instantaneous velocity fields of the axisymmetric turbulent impinging jet. The photograph of the jet flow is shown in Fig. 5. Large-scale vortex structures develop in the jet's mixing layer causing the PDF of the velocity fluctuations in a number of flow regions to be substantially non-Gaussian. Measurements have been performed with the aid of the 2D PIV Dantec FlowMap system with the use the simplest evaluation procedures (without advanced methods – adaptive correlation, window deformation, etc.) in order to provide a test in the most severe conditions. The details of the experimental installation and method are presented in the authors' work (Alekseenko et al., 2002).

Fig. 6 shows the convergence of the filtration algorithm the relative values of the statistical moments, calculated for each step, I, of filtration. It is obvious that at the first step the difference between non-filtered and true values is substantial. During filtration these values approach each other asymptotically. The lines 1, 2, 3 and 4 are, respectively, the mean value $\langle w\rangle/\langle w_{\text{true}}\rangle$, the variance $\sigma/\sigma_{\text{true}}$, the skewness factor S/S_{true} and the kurtosis E/E_{true}, for a chosen point in the jet mixing layer. Here index "true" means the asymptotic magnitudes.

The results of applying the proposed algorithm to PIV measurements in the axisymmetric turbulent impinging jet are presented in Fig. 7 for an ensemble of

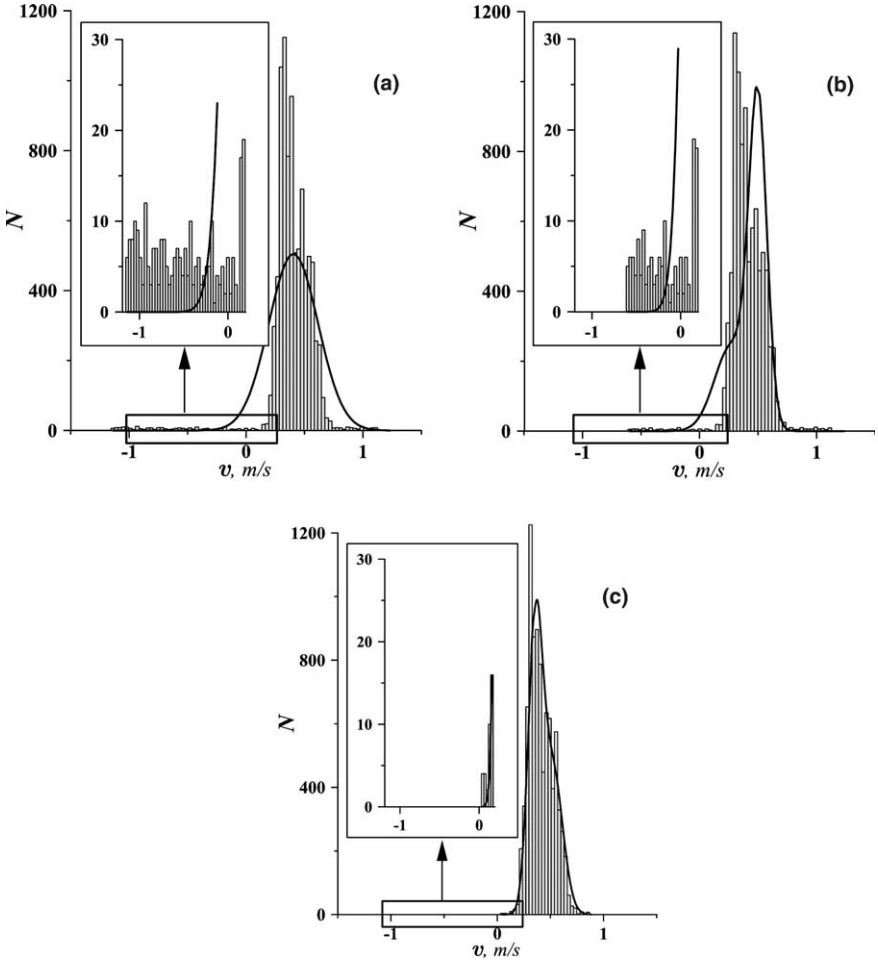

Fig. 9. Histograms and base functions for real experimental data, calculated at first (a), second (b) and last (c) iterations of filtration. Axisymmetric impinging jet, $H/D = 3$, $\mathscr{R}e = 7600$, $x = 0$, $y = 3.5$ mm.

instantaneous velocity fields consisting of 5000 realizations. For comparison, both non-filtered (a,c) and filtered (b,d) distributions of second and third statistical moments are shown. It is seen that the difference between non-filtered and filtered distributions grows rapidly with increasing order of the moment. The profiles of the first four moments measured at a distance of one diameter from the nozzle ($y/D = 2$, for coordinate system see Fig. 5) are presented in Fig. 8. Thus, the mean values and, in general degree, the variance of fluctuations are calculated correctly without any additional filtration (Fig. 8a and b). At the same time, the distributions of skewness and kurtosis are physically incorrect for the non-filtered case and differ from the true (filtered) values by several orders. As follows from the distributions, the statistical moments calculated for the filtered arrays are more correct and better reflect the physical nature of the impinging jet flow. It is important to note that the wrong vectors make the general contribution to errors in the calculated statistical moments in flow regions with large velocity gradients (jet mixing layer) and in the vicinity of the jet axis where longitudinal velocity fluctuations are very small and the PDF of velocity pulsations is rather narrow. The complete set of experiments processed with described filtration algorithm is presented in the authors' works (Alekseenko et al., 2002, 2003).

The proposed method has been also tested for the case where some important standard PIV-data validation steps are absent, i.e., peak validation and range validation. In such situations the proportion of non-physical vectors is extremely large (see Fig. 9a). Fig. 9b and c show the first and last step of filtration, respectively. It can be concluded that the filtration algorithm also works adequately for such conditions and that the final PDF does not contain any non-physical velocity fluctuations. The result of applying the proposed method under complicated conditions is presented in Fig. 10 where the distributions of the first three moments is plotted for non-filtered and filtered data. The distributions shown are taken along the axis of the impinging jet in the vicinity of the stagnation point. It is obvious that in this situation even the second moment is measured incorrectly with non-filtered values and some

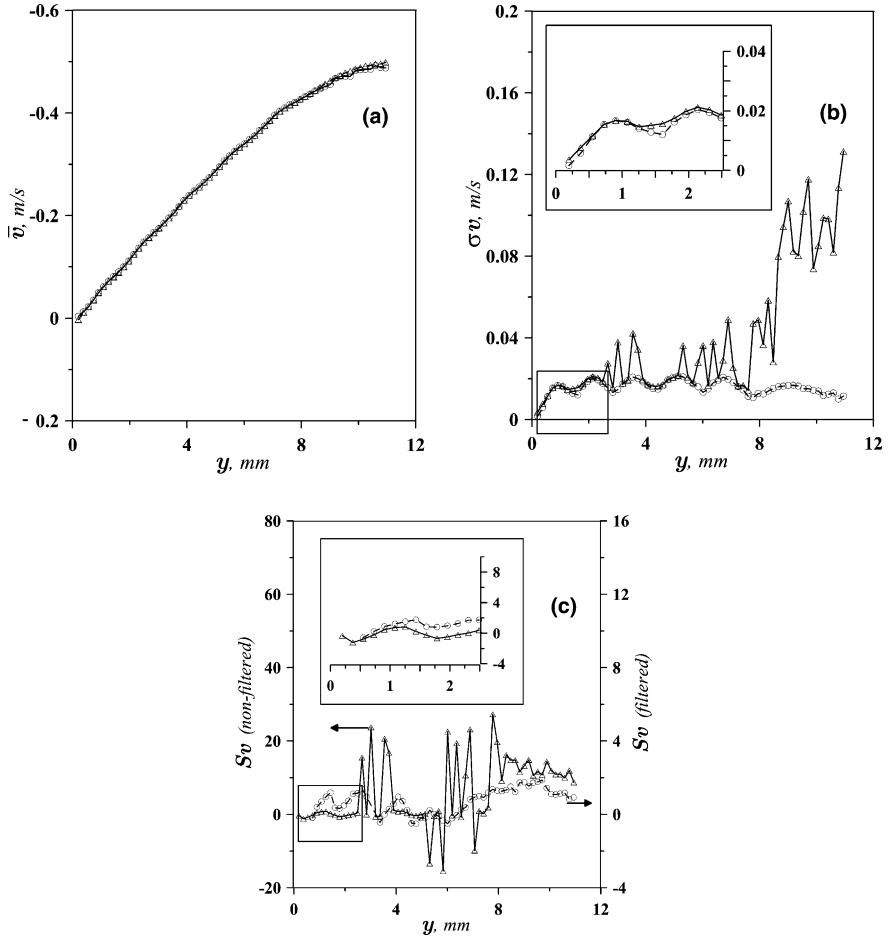

Fig. 10. Distributions of statistical moments across a vertical cross-section of the impinging jet flow ($x = 0$), $\mathscr{R}e = 7600$. (a) Mean longitudinal velocity, (b) its variance and (c) its skewness. Triangles—non-filtered values, circles—filtered values.

small deviations can even be observed for the mean velocity distribution ($y > 8$ mm).

The filtration algorithm is realized in the form of program code written in C++ language and has been built into a general package for acquisition, processing and analyzing data obtained by PIV-measurements. The developed code has been adapted for both two- and three-dimensional velocity fields.

6. Summary

A statistical method for filtering the ensemble of measured instantaneous velocity fields in turbulent flows has been developed and tested. The method is based on the assumption of an exponential decay of the PDF tails for velocity fluctuations in turbulent flows. The possibility of a substantial non-Gaussian character of PDFs for turbulent fluctuations has been taken into account. Such an approach allows the rejection of large-amplitude erroneous velocity vectors and hence makes possible the correct calculation of the higher order statistical moments. The testing of the algorithm was performed on the basis of generated artificial PDF's with imposed random noise. The developed method was then applied to the measured ensemble of instantaneous velocity fields in a turbulent impinging jet. The physically correct spatial distributions of statistical moments up to fourth order have been obtained.

Acknowledgements

This work was supported by RFBR grants N 04-02-16907 and 02-02-08081-inno.

References

Alekseenko, S.V., Bilsky, A.V., Heinz, O.M., Ilyushin, B.B., Markovich, D.M., 2003. Near-wall characteristics of impinging turbulent jet. Turbulence, Heat and Mass Transfer 4. In: Hanjalic, K., Nagano, Y., Tummers, M. (Eds.), Proceedings of Fourth International Symposium on Turbulence, Heat and Mass Transfer, Antalya, Turkey, October 12–17, 2003. pp. 235–241.

Alekseenko, S., Bilsky, A., Heinz, O., Ilyushin, B., Markovich, D., Vasechkin, V., 2002. Fine structure of the impinging turbulent jet. In: Rodi, W., Fueyo, N., (Eds.), Proceedings of the Fifth International Symposium on Engineering Turbulence Modelling and Experiments, Mallorca, Spain, September 16–18, 2002. pp. 597–606.

De Baas, A.F., van Dop, H., Nieuwstadt, F.T.M., 1986. An application of Langevin equation for inhomogeneous conditions to dispersion in a convective boundary layer. Q. J. R. Met. Soc. 112, 165–180.

Dekeyser, I., Launder, B.E., 1983. A comparison of triple-moment temperature-velocity correlations in the asymmetric heated jet with alternative closure models. In: Bradbury, L.J.S. et al. (Eds.), Turbulent Shear Flows, 4. Springer.

Ilyushin, B.B., 2001. Use of higher moments to construct pdf's in stratified flows. In: Launder, B.E., Sandham, N. (Eds.), Closure Strategies for Turbulent and Transitional Flows. Cambridge University Press, pp. 683–699.

Jovanovich, J., Durst, F., Johansson, T.G., 1993. Statistical analysis of the dynamic equations for higher order moments in turbulent wall-bounded flows. Phys. Fluids 26, 2886–2900.

Karlsson, R.I., Johansson, T.J., 1988. LDA measurements of higher order moments of velocity fluctuations in a turbulent boundary layer. In: Adrian, R., (Ed.), Laser Anemometry in Fluid Mechanics–III. Lisbon, Portugal. pp. 273–289.

Keck, T., 1978. Strukturelle Änderung von flüssigkeitsströmungen durch zugabe von hochpolumeren. Diplomarbeit, Institut für Hydromechanik, Universität Karlsruhe, pp. 135–138.

Panchapakesan, N.R., Lumley, J.L., 1993. Turbulence measurements in axisymmetric jets of air and helium. Parts 1 and 2. J. Fluid Mech. 246, 197–247.

Raffel, M., Willert, C., Kompenhans, J., 1998. Particle Image Velocimetry. A practical guide. Springer.

Tennekes, H., Lumley, J.L., 1972. A First Course in Turbulence. MIT Press, Cambridge, MA.